

# The vertical reservoir simulator CO<sub>2</sub>-VR

K. Piessens & M. Dusar

Royal Belgian Institute for Natural Sciences, Geological Survey of Belgium

## ABSTRACT

Geological reservoirs are usually horizontal structures with large horizontal dimensions and only a limited height. The general approach for modelling such reservoirs is to assume a constant density of the fluid that is injected or produced. This assumption is no longer valid when calculations are performed for reservoirs with a large vertical extent, up to several hundred meters, or for fluids that are near critical or near saturated. A typical coal mine has a large vertical dimension that far exceeds the 100 m range. When it would be used for CO<sub>2</sub>-sequestration, the pressure and temperature conditions would be close to the saturation conditions of CO<sub>2</sub> or its super-critical extension. In order to calculate the reservoir conditions in detail, the one-dimensional vertical reservoir simulator CO<sub>2</sub>-VR was developed.

The simulator calculates the reservoir pressures and densities for CO<sub>2</sub> at each depth. Calculation therefore starts from a point for which the reservoir pressure is known. Using this data, the pressure conditions of the cells above and below the starting cell are estimated in an upward-downward calculation scheme. This approach produces pressure and density profiles that are in equilibrium with a given geothermal gradient. Simulation shows that inside a reservoir filled with CO<sub>2</sub> large density differences may occur. The most extreme cases predict unstable situations with liquid-like CO<sub>2</sub> occurring at the top and gas-like CO<sub>2</sub> at the bottom of the reservoir.

These data are used to calculate the storage capacity of the reservoir in the non-flooded parts (density of CO<sub>2</sub>), the flooded parts (solubility calculations based on temperature, pressure and salinity), and adsorbed to coal (adsorption data based on pressure, temperature and coal type). Extended features allow calculating the effect of pressurising the reservoir and of the amount of heat that can be produced by CO<sub>2</sub>-geothermics.

## INTRODUCTION

The density of a fluid changes with depth due to pressure, temperature and changes in composition. An example of this is the, be it modest, increase of the density of most formation waters with depth. The same principle also applies to oil or natural gas reservoirs, but since most reservoirs are dominantly horizontal structures, differences in density can usually be neglected.

This simplification is not necessarily valid for reservoir types such as an abandoned mine that may have a vertical extent of several hundreds of metres. In order to correctly assess the possibility of CO<sub>2</sub>-sequestration in abandoned coal mines, a static, one-dimensional simulator was created to take into account the effects of density changes of pure CO<sub>2</sub> with depth.

## COAL MINE RESERVOIR

A coal mine reservoir differs from most geological reservoirs, such as aquifers and depleted oil fields, for several reasons. Classical reservoirs are usually flat and horizontal structures, whereas a mine is irregular and has a large height. Also the permeability of such a reservoir, even if completely collapsed, is very high compared to the natural pre-mining state. The modes of sequestration are also typical. In a coal mine, CO<sub>2</sub> can be stored in 'free-space' (gas-filled parts), in solution in mine water, and/or adsorbed to coal reserves. However, coal mines suited for CO<sub>2</sub>-sequestration are non-flooded, well-sealed structures [1]. The initial pressure in such a reservoir will therefore be low (close to atmospheric). This means that the initial pressure-state is in dramatic disequilibrium with the hydrostatic pressure gradient. These aspects hinder the use of standard reservoir simulators when assessing CO<sub>2</sub>-sequestration in mine reservoirs.

Therefore an independent calculation scheme was set up to calculate the static-state conditions just after injection and at maximum pressure condition. The model is based on two important assumptions. The first is that the permeability of the reservoir, even in the collapsed parts, is sufficiently high (estimates for the gallery network around 1000 darcy and higher [2]) to allow considering the mine as one continuous reservoir. In practise this means that horizontal levels will be in equilibrium. Therefore the complex geometry of the mine can be simplified to a one-

dimensional model and no time considerations have to be made for the migration of injected CO<sub>2</sub> through the reservoir (fig. 1).

Secondly the model assumes that the top and bottom seals are perfect, and that flooding occurs according to a theoretical worst-case scenario, depicted in fig. 2. First situation is the initial situation (fig. 2a), assuming the current level of flooding (mine is dry in fig. 2a) and free-space filled with CO<sub>2</sub>. Because of the density difference between CO<sub>2</sub> and H<sub>2</sub>O, the pressure at the bottom of the reservoir will be lower than the hydrostatic pressure that prevails in the host rocks, although this is not necessarily true at higher levels in the reservoir (fig. 3). As a result, formation water will enter the reservoir (fig. 2b). Usually this will be a slow process because suitable coal mines are hosted by relatively impermeable strata. The rise of the mine water (formation water) will compress CO<sub>2</sub>, and as a result pressure build-up will occur at the top of the reservoir. Eventually, even if this is not the case in the initial situation, reservoir pressures higher than hydrostatic will be reached at the top of the reservoir. As a result, CO<sub>2</sub> will migrate out of the reservoir. This flux is however neglected, as its relative importance in non-permeable host-rock is difficult to estimate, and instead a worst-case scenario (maximum pressure build-up) is calculated. The influx of formation water will continue until the pressure at each level of the reservoir filled with CO<sub>2</sub> is higher than the hydrostatic pressure (fig. 2c). The pressure in the flooded parts of the reservoir always remains in equilibrium with the hydrostatic gradient. A safe reservoir should withstand the reservoir pressure at this stage, which may be significantly higher than the initial reservoir pressure. Reservoirs with a leak-off pressure lower than the hydrostatic pressure are for this reason not suitable for CO<sub>2</sub>-sequestration. They may however be used for short-term gas storage, provided that the reservoir is maintained by evacuating excess of mine water [1]. CO<sub>2</sub>-VR is capable of predicting the maximum pressure conditions from a given initial situation, or calculating the maximum allowed amount of CO<sub>2</sub> to be injected in the initial situation, given the maximum allowed reservoir pressure.

The maximum pressure condition (fig. 2c) is not an equilibrium condition, since the reservoir pressure is higher than the hydrostatic pressure in the host rocks. Therefore CO<sub>2</sub> will escape from the reservoir and migrate laterally into the host formation (fig. 2d). This will result on long term in a near complete flooding of the mine (fig. 2e), but does not violate the terms for sequestration because CO<sub>2</sub> will remain trapped by the top seal.

## SOFTWARE ENVIRONMENT AND CALCULATION SCHEME

The current version of this program has been created using Microsoft Excel in combination with Visual Basic for Applications. This approach was chosen because focus had to be on the structure and evaluation of the calculation scheme, rather than on performance. Due to lookup functions in combination with a large database and the use of recursive formulas, the calculation speed is currently rather low. A normal calculation may take up to 15 minutes, whereas backward or iterative computations are usually conducted overnight.

The grid consists of a one-dimensional series of 100 cells. Each cell represents a certain depth interval of the mine. Properties are assigned either directly, as for residual volume, or are calculated from user-entered parameters, as for example the geothermal gradient (Fig. 4). In this way, each cell is assigned a value for depth, temperature, residual volume, salinity of mine water, hydrostatic gradient, type and amount of coal, and so on. The primary parameters in the calculation scheme are density and pressure. This requires the following general parameters: the amount of CO<sub>2</sub> in the reservoir, or the reservoir pressure at a certain depth. Usually the reservoir pressure is chosen, either as the maximum allowed reservoir pressure at the top of the reservoir or as the hydrostatic pressure at a certain depth, defining which part of the reservoir remains unflooded. At this level of flooding, both pressure and temperature are known, and therefore the density of CO<sub>2</sub> can be calculated for this cell. This density is used to calculate the pressure in the overlying and underlying cells, assuming a CO<sub>2</sub>-static gradient. This is the basis for a recursive procedure that allows the calculation of the whole density profile in an upward-downward scheme. If the amount of CO<sub>2</sub> in the reservoir is entered instead of pressure, then the same calculation scheme is run in an iterative procedure to determine the reservoir pressure. The CO<sub>2</sub> static density and pressure gradients are compared with the hydrostatic gradient of the mine water. Cells where the CO<sub>2</sub>-static pressure is higher than the hydrostatic pressure are considered to be filled with CO<sub>2</sub> and vice versa. For CO<sub>2</sub> filled cells, free-space parameters such as storage capacity, adsorption on dry coal and condensation heat are calculated. For cells representing the flooded parts of the mine, the solution storage capacity and adsorption on wet coal are computed. All these secondary results can be calculated directly from the cell properties. Finally the cell results are summarised by calculating total and average values for the whole mine.

## PROPERTIES OF PURE CO<sub>2</sub>

The final composition of the reservoir fluid will be dominated by CO<sub>2</sub> with probably minor amounts of e.g. CH<sub>4</sub>, N<sub>2</sub> and H<sub>2</sub>O, although the exact composition may be difficult to predict. The temperature and pressure conditions in most mine reservoirs will be close to critical, and therefore it is important to use equations of state (EOS) that also accurately describe the non-ideal behaviour of fluids. These currently do not exist for gas mixtures and therefore the reservoir fluid is considered to contain pure CO<sub>2</sub> only. The CO<sub>2</sub>-EOS of [3] is used to calculate the mono-phase pressure, temperature and density properties of CO<sub>2</sub>, along with the Gibbs-free energy which is used to estimate the geothermal potential. This equation is stated to be reliable down to the critical point. CO<sub>2</sub>-VR contains a database that was extracted from the NIST-database [4] tabulating the pressure of CO<sub>2</sub> for densities between 10 and 1000 kg/m<sup>3</sup> and for temperatures between -56 and +1000 °C, incrementing with 10 kg/m<sup>3</sup> and 0.1 °C respectively. Data is extracted from this database using linear interpolation between the closest matching data points. This method makes it possible to calculate the density of a cell that contains both liquid and gaseous CO<sub>2</sub>.

For H<sub>2</sub>O there is a simple relation between the water depth and pressure, but this is not true for CO<sub>2</sub> because density and pressure profiles of CO<sub>2</sub> can not be assumed to vary linearly with depth. Therefore, and because of the mathematically complex EOS, the use of a recursive algorithm is necessary to calculate the pressure and densities of CO<sub>2</sub> throughout the reservoir. It is the calculation of the density profile that is the primary reason why CO<sub>2</sub>-VR has been developed. The temperature is considered to be in equilibrium with the geothermal gradient in the host rock [1], except for the calculation of the geothermal potential, where the temperature profile is changed until the density of CO<sub>2</sub> at all depths is constant.

An example of a reversed density profile from an assessment study for the Belgian Beringen colliery [1] is given in fig. 8. Note that at the top of the reservoir CO<sub>2</sub> has a density comparable to liquid CO<sub>2</sub>, whereas at the deepest level, it would be gas like. Simulators that do not take into account a variable density of CO<sub>2</sub> will produce erroneous results. CO<sub>2</sub>-VR is only capable of calculating the static state of a reservoir, but it is clear that these density differences in a reservoir with a high permeability will lead to convection currents and a redistribution of the temperature profile.

## SOLUBILITY OF CO<sub>2</sub> IN MINE WATER

CO<sub>2</sub> is characterised by a relatively high solubility in pure water due to the hydration of CO<sub>2</sub>. Basically, an increase in pressure will increase the solubility, whereas increased salinity has the opposite effect. The latter is referred to as the salting-out effect. An increase in temperature may either increase or decrease solubility, depending on the prevailing pressure (cf. [5]). However, the competing effects of pressure, temperature and salinity generally result in an increasing solubility of CO<sub>2</sub> in formation waters with depth.

The solubility of CO<sub>2</sub> in aqueous solutions has been studied up to temperatures of 450 °C, pressures of 140 MPa and in solutions of NaCl, CaCl<sub>2</sub> and in brines ([5], [6], [7], [8] and [9]). Several equations have been proposed that can be reduced to the same basic format (App. A):

$$m = \frac{\Phi \cdot (P - p_w)}{K_H \cdot k_T \cdot k_s \cdot e^{\frac{v \cdot (P - p_w)}{R \cdot T}}} \quad (1)$$

In this equation, pressure (P) and temperature (T) are known values for each grid-cell and the value of the universal gas constant (R) is accurately known. For the other parameters, several authors propose different values and approximations. The partial pressure of water was estimated from the regression of [10] which is valid over a larger temperature range than the ones proposed by [4]. The fugacity coefficient (Φ) is temperature dependent. It is empirically known for pure H<sub>2</sub>O and CO<sub>2</sub>, from which [11] estimated the fugacity coefficient for the mixed system. Their tabulated results were matched by a square regression curve (difference for individual points < 1 %). Approximations for Henry constant (K<sub>H</sub>), defined at standard P-T-conditions and infinite dilution, are summarised by [12] (values from 16 different authors) and given by [8] and [6]. [7] and [13] provide Henry constants that are only valid at higher temperatures, pressures or in salt-containing solutions. Most authors provide activity coefficients correcting K<sub>H</sub> for temperature (k<sub>T</sub>), only those of [8], [6], [7] and [13] are stated to be applicable at sufficient high temperatures. An activity coefficient for the salting out effect (k<sub>s</sub>) is given by [6], [7] and [13].

Estimates of the partial molar volume of CO<sub>2</sub>, used to correct the Henry coefficient for non-standard pressure conditions with the Peng-Robinson equation of state:

$$k_p = e^{\frac{v(P-p_w)}{RT}} \quad (2)$$

were taken from [14], [7] and [13]. In order to choose the most accurate set of equations and to determine their accuracy, all combinations of values and sub-equations have been tested against a dataset that contains 82 measurements of the solubility of CO<sub>2</sub> in water for temperatures ranging from 0 to 200 °C, pressures between 0.1 and 20 MPa and salinities up to 1 wt% NaCl or 22 wt% CaCl<sub>2</sub>. The most accurate set of equations is given in appendix A and used by CO<sub>2</sub>-VR. It gives reliable predictions between 25 and 200 °C, below 10 MPa for salt-free systems, and between 50 and 200 °C, below 10 MPa at all salinities. Error analysis indicates an accuracy that is generally better than 10 % or 2 g/kg (largest of the two values). The reliability of this interval is about 95 % for salt-containing systems and better for salt-free systems. In CO<sub>2</sub>-VR the solubility is expressed in kg of CO<sub>2</sub> per m<sup>3</sup> solution, and can thus easily be compared to the free-space storage capacity.

### ADSORPTION OF CO<sub>2</sub> ON COAL

An important amount of CO<sub>2</sub> injected in a coal mine will be adsorbed on remaining coal reserves. Substantial efforts are being undertaken to accurately establish the adsorption properties of natural coal for CO<sub>2</sub>, however this has not yet led to accurate equations of state (e.g. [15]). Therefore CO<sub>2</sub>-VR makes estimates based on the adsorption capacity of active coal. Data at 0 to 80 °C and up to 6 MPa for dry active coal ([16], [17] and [18]) were fitted to a temperature dependent dual-site Langmuir adsorption isotherm using a multi-variant approach, and assuming a linear relation of the 8 calibrated parameters with temperature (fig. 5). Note that the calibration range is limited and important extrapolations have to be made. The adsorption capacity of active coal is higher than this of natural coal because of its higher internal surface and its composition. The former effect is taken into account by introducing a factor that is equal to the ratio of the internal surface of natural coal to the internal surface of active coal. Usually this is around 0.3 ([19], [20] and [21]), implying that this effect alone will reduce the adsorption capacity to one third. The influence of compositional variations is evident from the data obtained on natural coal samples [16]. These data have been normalised to the adsorption capacity of active coal at the same pressure and temperature, and show a relation with the volatile matter content (fig. 6). The latter parameter is well known for most coal mines, and can therefore be used to estimate the factor needed to estimate the adsorption on natural coal, relative to the adsorption on active coal. Humidity reduces the adsorption capacity of coal. Reported values for changes in CH<sub>4</sub>-adsorption are a reduction of 25 % [22], resulting from 1 % humidity, and a reduction of 50 %, resulting from total water saturation. A well-documented reduction of 65 % due to total saturation with water for adsorption of CO<sub>2</sub> on coal from the Belgian Beringen colliery has been reported by [23], [24] and [25], but values for other samples may vary significantly.

Using all of these evaluations, it is possible to estimate, to some extent, the adsorption capacity of coal remaining as reserves in a coal mine. This is a very indirect approach and the available calibration data are insufficient. This clearly leads to inaccuracies, as is shown by the comparison with the measured excess sorption data of [15] (fig. 7). However, the main source of error does not lie in the assessment of the adsorption capacity of a specific type of coal, but on the estimation of the amount of coal available for adsorption in a coal mine. In general the coal reserves, still in place at the time of abandonment of a mine, are to some extent known and in some cases also their depth and location, but only a fraction of this reserve will actually participate in the adsorption of CO<sub>2</sub>. Therefore in many cases only a general figure will be calculated and fed into CO<sub>2</sub>-VR. Only in a limited number of cases will the available data be sufficient to allow the calculation of the adsorption profile.

### CONCLUSION

CO<sub>2</sub>-VR is currently a stand-alone program that is capable of predicting static reservoir conditions that can be used to accurately evaluate the use of abandoned coal-mines as reservoirs for CO<sub>2</sub>-sequestration. In spite of the rudimentary nature of CO<sub>2</sub>-VR, it is able to produce accurate and reliable results. One striking conclusion is that the rule of thumb that CO<sub>2</sub> will be supercritical below ~800 m and gas-like at shallower depths, is not applicable to coal mine reservoirs, but that on the contrary CO<sub>2</sub> at shallow depths will be denser than at deeper levels. This unstable situation will result in convection, especially when the reservoir has a large vertical extent. In order to model such

reservoir dynamics, CO<sub>2</sub>-VR will in future be translated in a faster code and coupled to other reservoir simulators. Results of the dynamic simulation will be of interest for the accurate prediction of CO<sub>2</sub>-sequestration projects, but also for the dimensioning of the concept of CO<sub>2</sub>-geothermics that is based on the enhanced circulation of CO<sub>2</sub> in a permeable reservoir [26].

#### APPENDIX: SYMBOLS, UNITS AND EQUATIONS

$m$  molality of CO<sub>2</sub> in solution (g<sub>CO<sub>2</sub></sub>/kg<sub>H<sub>2</sub>O</sub>)

$\Phi$  fugacity coefficient (dimensionless)

$P$  pressure (MPa)

$p_w$  partial pressure of water (MPa)

$K_H$  Henry constant at standard conditions (0.1 MPa and 25 °C) and infinite dilution (MPa.kg<sub>H<sub>2</sub>O</sub>/g<sub>CO<sub>2</sub></sub>; [7], eq. 4):

$$K_H = \frac{-5032.99 + 30.74113 \cdot T - .052667 \cdot T^2 + 2.630218 \cdot 10^{-5} \cdot T^3}{55.3} \quad (3)$$

$$= 2.64 \frac{\text{MPa.kg}_{H_2O}}{g_{CO_2}} \quad \text{at } 25^\circ\text{C}$$

$k_T$  activity coefficient, correction  $K_H$  for non-standard temperatures (dimensionless; [7], eq. 4):

$$k_T = \frac{\left( -5032.99 + 30.74113 \cdot T - .052667 \cdot T^2 + 2.630218 \cdot 10^{-5} \cdot T^3 \right)}{K_H} \quad (4)$$

$$\cdot \frac{\left( 1 - \frac{\phi \cdot (P - p_w)}{-5032.99 + 30.74113 \cdot T - .052667 \cdot T^2 + 2.630218 \cdot 10^{-5} \cdot T^3} \right) \cdot .0180153}{K_H}$$

$k_s$  activity coefficient, correction  $K_H$  for presence of salts (dimensionless; [7]):

$$k_s = \frac{1}{1 - 0.04893414 \cdot \text{TDS} + 0.001302838 \cdot \text{TDS}^2 - 0.00001871199 \cdot \text{TDS}^3} \quad (5)$$

$\text{TDS}$  total dissolved solids concentration, excluding dissolved gases (wt%)

$v$  partial molar volume of CO<sub>2</sub> (cm<sup>3</sup>/mol; [14]):

$$v = 77.8325585278782 - 0.327883964055375 \cdot T + 0.000594831435589504 \cdot T^2 \quad (6)$$

$R$  universal gas constant (MPa.cm<sup>3</sup>/(mol.K))

$T$  temperature (K)

#### REFERENCES

1. Piessens K. and M. Dusar, 2003: "CO<sub>2</sub>-sequestration in abandoned coal mines"; this volume.
2. van Tongeren P.C. and B. Laenen, 2001: "Residual space volumes in abandoned subsurface coalmines of the Campine Basin (northern Belgium)" Vito-report ordered by NITG-TNO, GESTCO 3, 38 p.
3. Span R. and W. Wagner, 1996: "A new equation of state for carbon dioxide covering the fluid region from the triple point temperature to 1100 K at pressures up to 800 MPa"; Journal of physical and chemical reference data, V. 25, p. 1509-1596.

4. Lemmon E.W., M.O. McLinden and D.G. Friend, 2001: "Thermophysical properties of fluid systems"; NIST chemistry webbook, NIST standard reference database 69, eds. Linstrom P.J. & Mallard W.G., National Institute of Standards and Technology, Gaithersburg, <http://webbook.nist.gov>.
5. Takenouchi S. and G.C. Kennedy, 1965: "The solubility of carbon dioxide in NaCl solutions at high temperatures and pressures"; *American Journal of Science*, V. 263, p. 445-454.
6. Barta L. and D.J. Bradley, 1985: "Extension of the specific interaction model to include gas solubilities in high temperature brines"; *Geochimica et Cosmochimica Acta*, V.49, p. 195-203.
7. Enick E. and S.M. Klara, 1990: "CO<sub>2</sub> solubility in water and brine under reservoir conditions"; *Chem. Eng. Comm.*, V. 90, p. 23-33.
8. Rumpf B. and G. Maurer, 1993: "An experimental and theoretical investigation on the solubility of carbon dioxide in aqueous solutions of strong electrolytes"; *Ber. Bunsenges. Phys. Chem.*, V. 97, p. 85-97.
9. Holloway S., 1996: "The underground disposal of carbon dioxide"; Final report of the JOULE II project No. CT92-0031, ed. Holloway S., 355 p.
10. Saul A. and W. Wagner, 1987: "International equations for the saturation properties of ordinary water substance"; *J. Phys. Chem. Ref. Data*, V. 16, p. 893-901.
11. Hayden J.G. and J.P. O'Connell, 1975: "A generalized method for predicting second virial coefficients"; *Ind. Eng. Chem. Proc.*, V. 14, p. 209-216.
12. Sander S.A., 1999: "Compilation of Henry's Law Constants for Inorganic and Organic Species of Potential Importance"; *Environmental Chemistry (Version 3)*, <http://www.mpch-mainz.mpg.de/~sander/res/henry.html>.
13. Nighswander J.A. and N. Kalogerakis and A.K. Mehrotra, 1989: "Solubilities of carbon dioxide in water and 1 wt % NaCl solution at pressures up to 10 MPa and temperatures from 80 to 200 °C"; *J. Chem. Eng. Data*, V. 34, p. 355-360.
14. Brelvi S.W. & O'Connell J.P. 1972. Corresponding states correlation for liquid compressibility and partial molar volumes of gases at infinite dilution in liquids. *AIChE-J*, 18, p. 1239-1243.
15. Krooss B.M., F. van Bergen, Y. Gensterblum, N. Siemons, H.J. Pagnier and P. David, 2002: "High-pressure methane and carbon dioxide adsorption on dry and moisture-equilibrated Pennsylvanian coals"; *International Journal of Coal Geology*, V. 51, p. 69-92.
16. Coppens P.J., 1967: "Synthèse des propriétés chimiques et physiques des houilles. Les houilles belges"; Report of the Institut national de l'industrie charbonnière, publ. by Inichar, 216 p.
17. Dreisbach F., R. Staudt and J.U. Keller, 1999: "High pressure adsorption data of methane, nitrogen, carbon dioxide and their binary and ternary mixtures on activated carbon"; *Adsorption*, V. 5, p. 215-227.
18. van der Vaart R., C. Huiskens, H. Bosch & T. Reith, 2000: "Single and mixed gas adsorption equilibria of carbon dioxide/methane on activated carbon"; *Adsorption*, V. 6, p. 311-323.
19. Van Krevelen D.W., 1963: "Geochemistry of coal"; *Organic geochemistry*, Ed. Breger I.A., monograph 16, Earth Sciences, p. 183-247.
20. Van Krevelen D.W., 1993: *Coal: the Netherlands*, Amsterdam, Elsevier Science Publishers.
21. Norit, 2002: "Activated carbon technical information"; [www.norit.com](http://www.norit.com).
22. Houtrelle S., 1999: "Stockage de gaz naturel en mine de charbon abandonnée. Approche géologique du site d'Anderlues"; Faculté polytechnique de Mons, Master thesis, 50 p.
23. Haan M.F.E., 1998: "Enhanced coalbed methane production by carbon dioxide injection; theory, experiments and simulations"; Master thesis, TU-Delft, faculty of applied Earth sciences, 82 p.
24. Bertheux W.B., 2000: "Enhanced coalbed methane production by carbon dioxide injection in water saturated coal; experiments, image analysis and simulations"; Master thesis, TU-Delft, faculty of applied Earth sciences, 112 p.
25. Hamelinck C.N., A.P. Faaij, G.J. Ruijg, D. Jansen, H. Pagnier, F. van Bergen, K.-H. Wolf, O. Barzandji, H. Bruinig and H. Schreurs, 2001: "Potential for CO<sub>2</sub> sequestration and enhanced coalbed methane production in the Netherlands"; Novem report, 105 p.
26. Piessens K. and M. Dusar, 2003: "CO<sub>2</sub>-geothermics in abandoned coal mines"; this volume.

## FIGURES

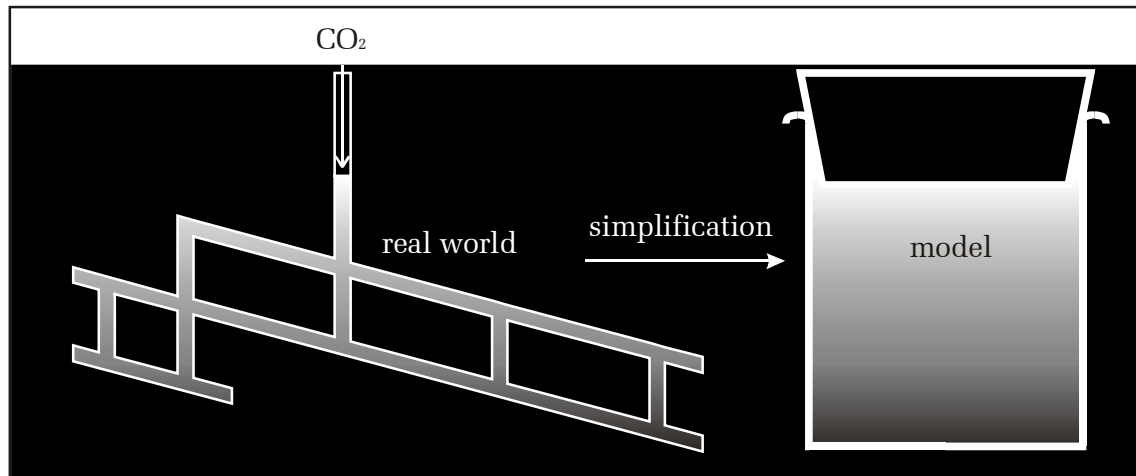


Figure 1:

Schematic representation of the complex geometry of a coal mine. Due to the very high permeability, CO<sub>2</sub> will quickly migrate through the reservoir. Therefore horizontal equilibrium is assumed at all times and only vertical (one-dimensional) calculations are made.

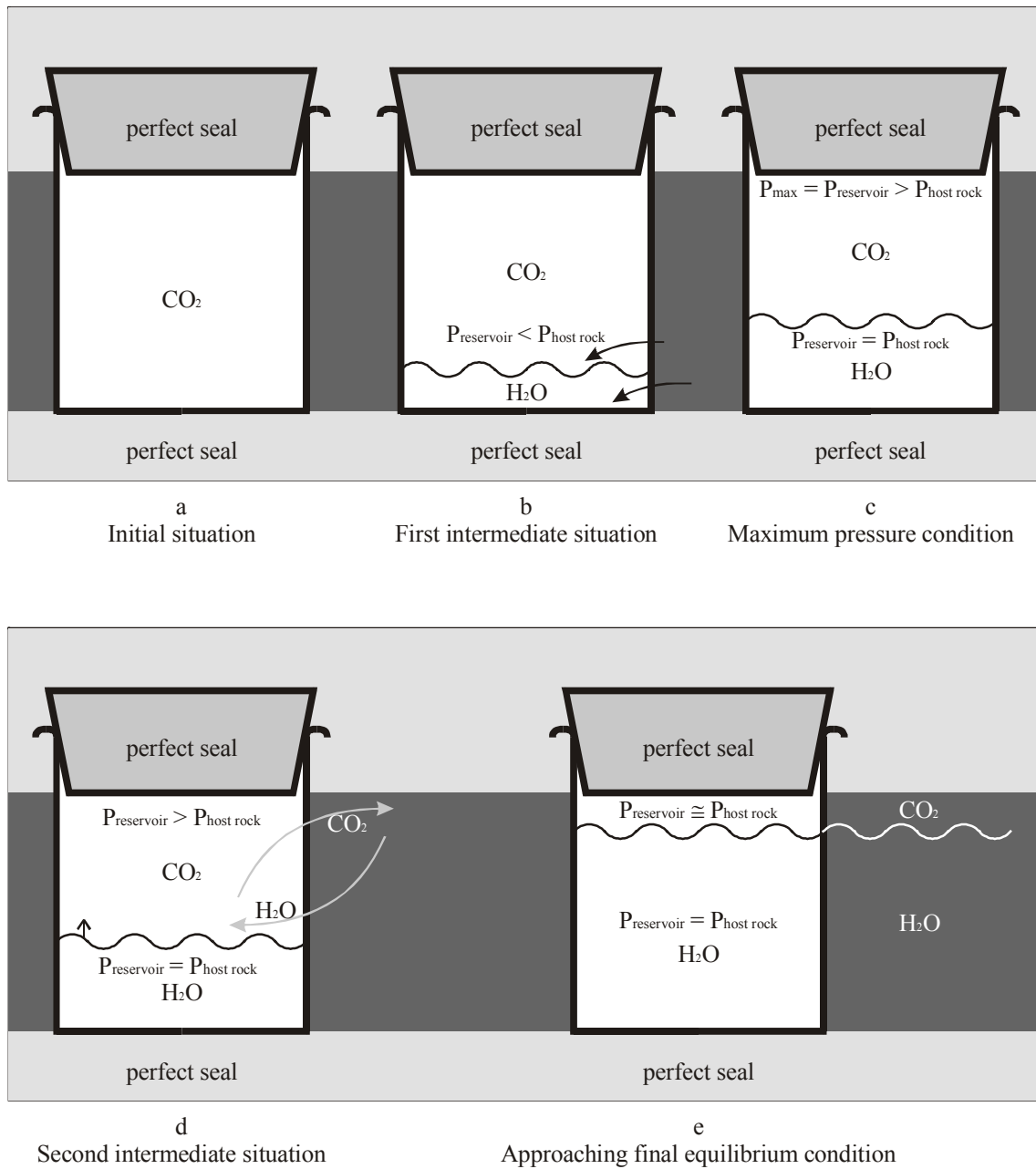


Figure 2:

Cartoons representing the evolution of a mine reservoir as assumed by CO<sub>2</sub>-VR. CO<sub>2</sub> is assumed to be perfectly sequestered in stages a to c. The calculated maximum reservoir pressure will therefore be higher than the true expected pressure. See text for detailed discussion.

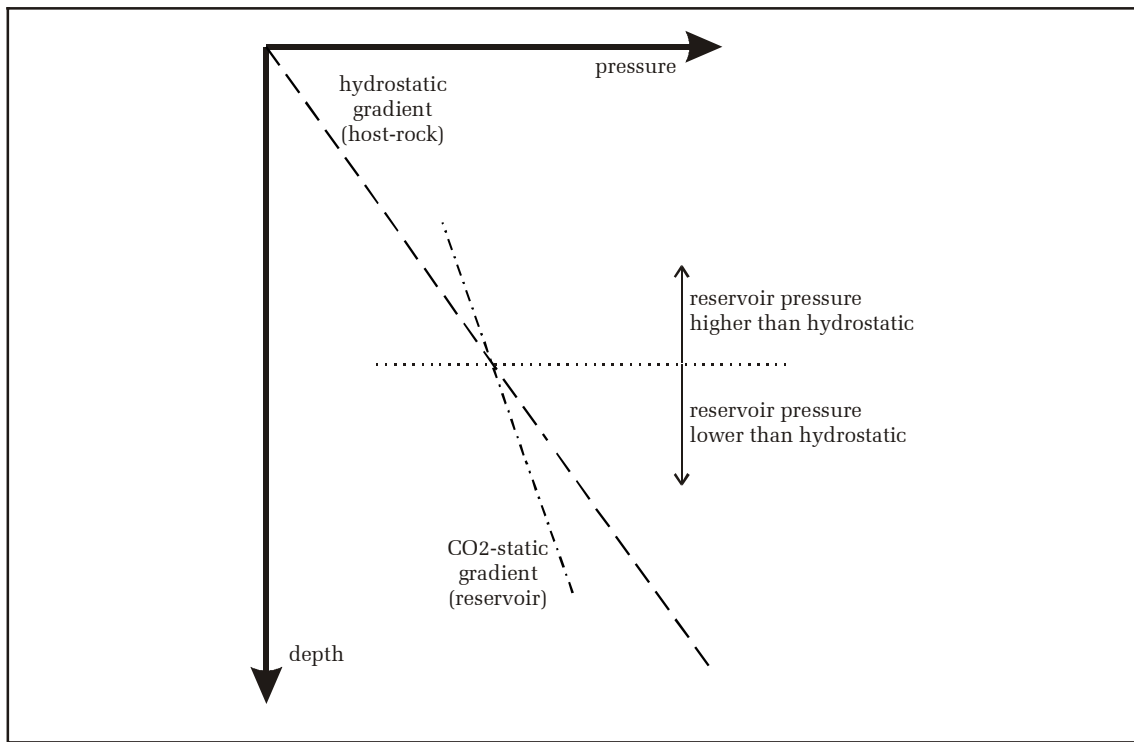


Figure 3:

The pressure gradient in the reservoir is determined by  $\text{CO}_2$ , whereas in the host rock it approximates the hydrostatic gradient. This results in pressure disequilibrium due to the different densities of  $\text{H}_2\text{O}$  and  $\text{CO}_2$ .

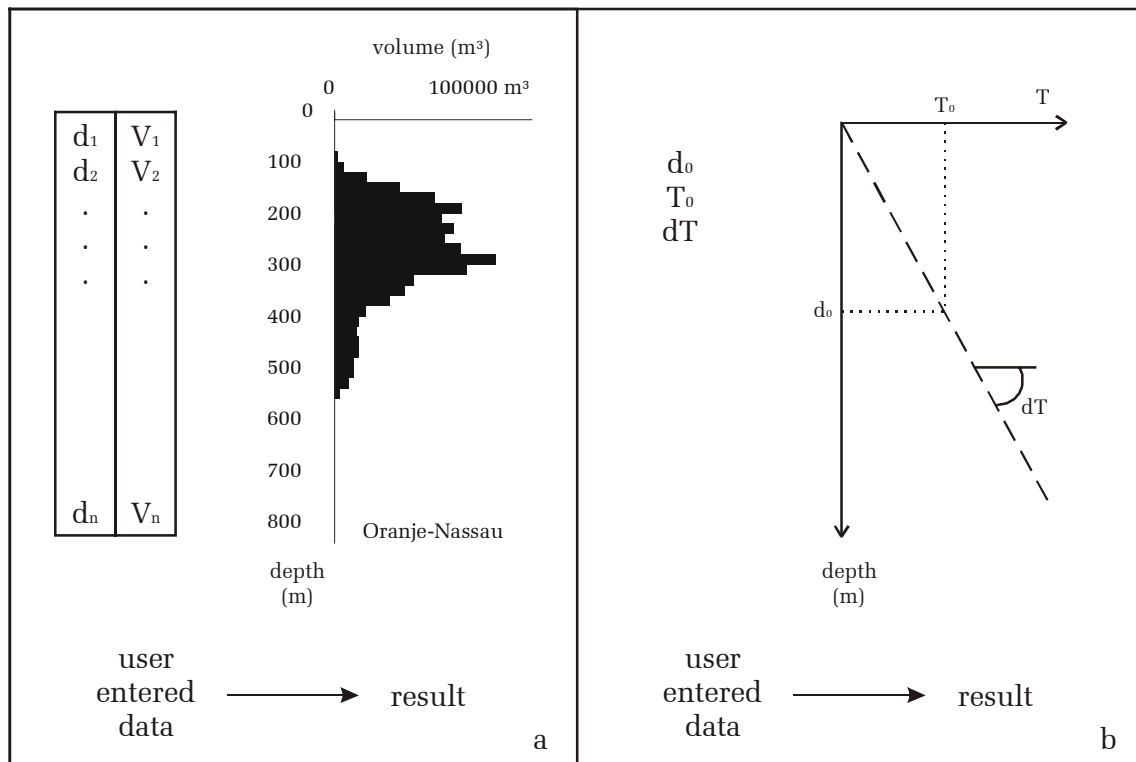


Figure 4:

Data in CO<sub>2</sub>-VR is entered either (a) by manually assigning a value to each cell, as is required for the residual space distribution (data from the Oranje-Nassau mine, The Netherlands, source: VITO, Belgium), or (b) by defining parameters describing a gradient, as is shown for the linear geothermal gradient.

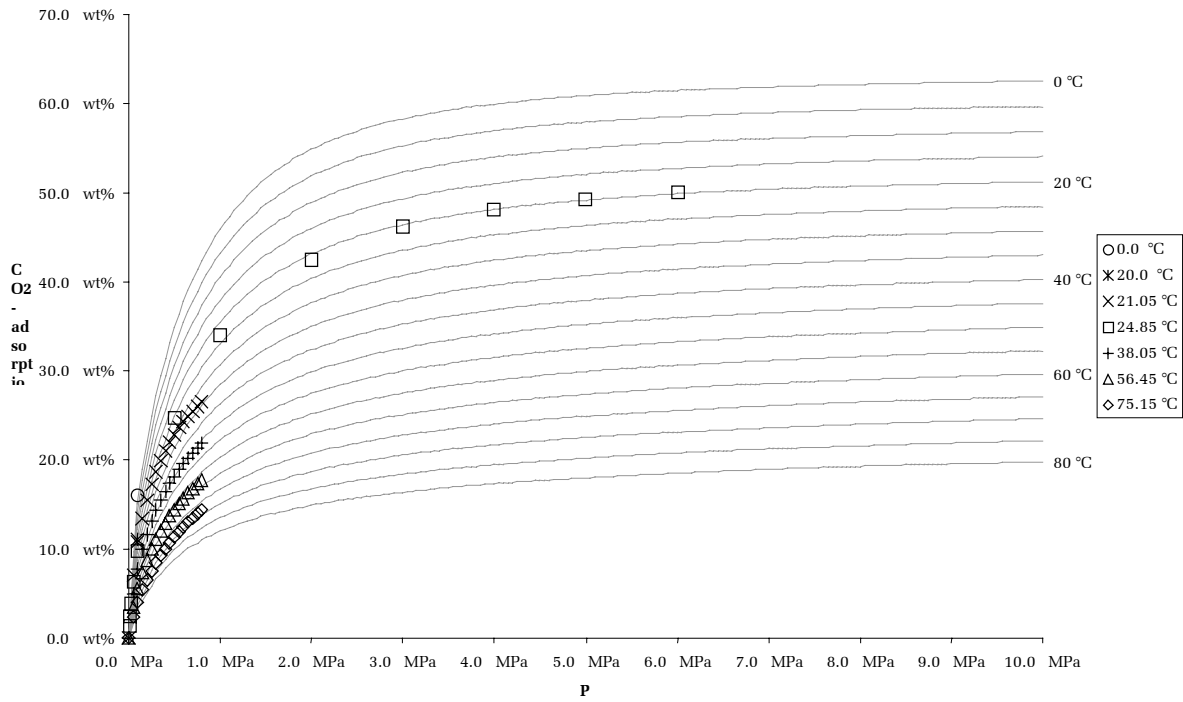


Figure 5:

Temperature dependence of the adsorption characteristics of CO<sub>2</sub> on active coal (Norit), modelled using the dual-site Langmuir adsorption criterion and assuming linear relationship of the temperature dependent parameters. Data from [16], [17] and [18].

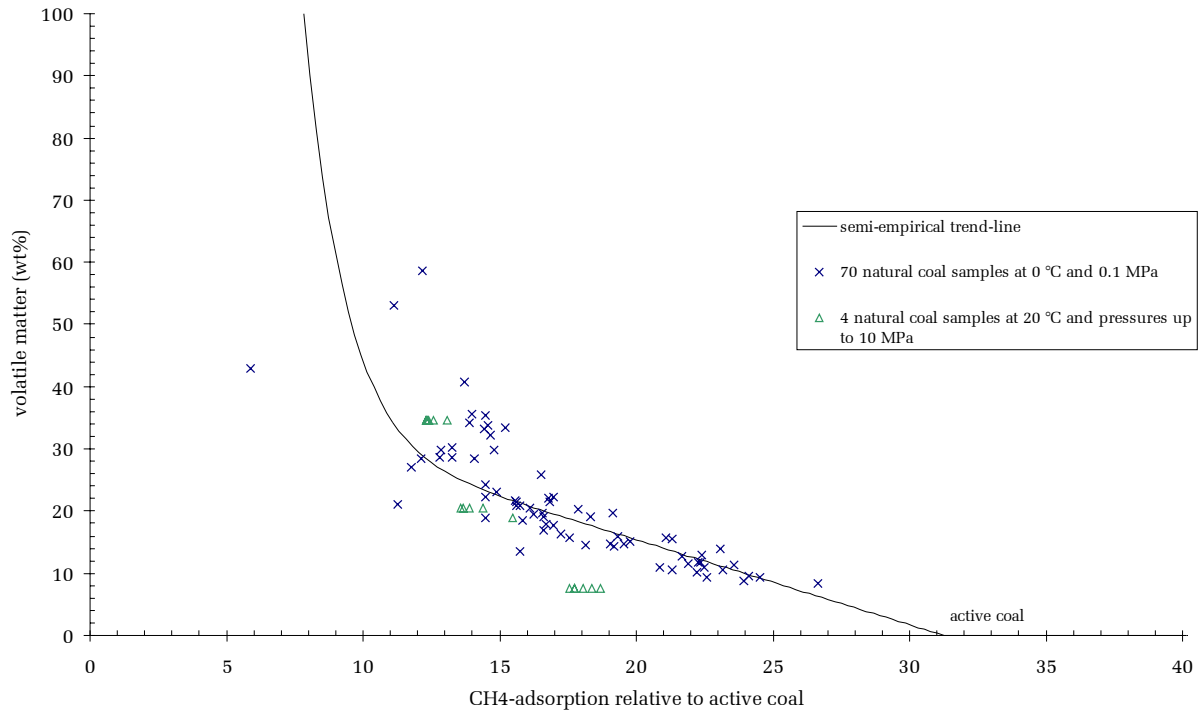


Figure 6:

Relation between the maximum adsorption of CH<sub>4</sub> on natural coal samples, relative to active coal (Norit) at the same pressure conditions, and the content of volatile matter (maceral content), being 0 for active coal. Volatile matter given for ash-free and dry samples. Adsorption values for 20 °C were recalculated to probable values at 0 °C. The semi-empirical trend line is based on geometrical and probability considerations. The data from [16] best fit the trend-line when an average value of 3.2 is assumed for the ratio between the surface of activated carbon and natural coal. This is why the point for active coal is located at the X-axis near 31 % instead of 100 %. The ratio of 3.2 is in agreement with estimated internal surfaces ([19], [20] and [21]).

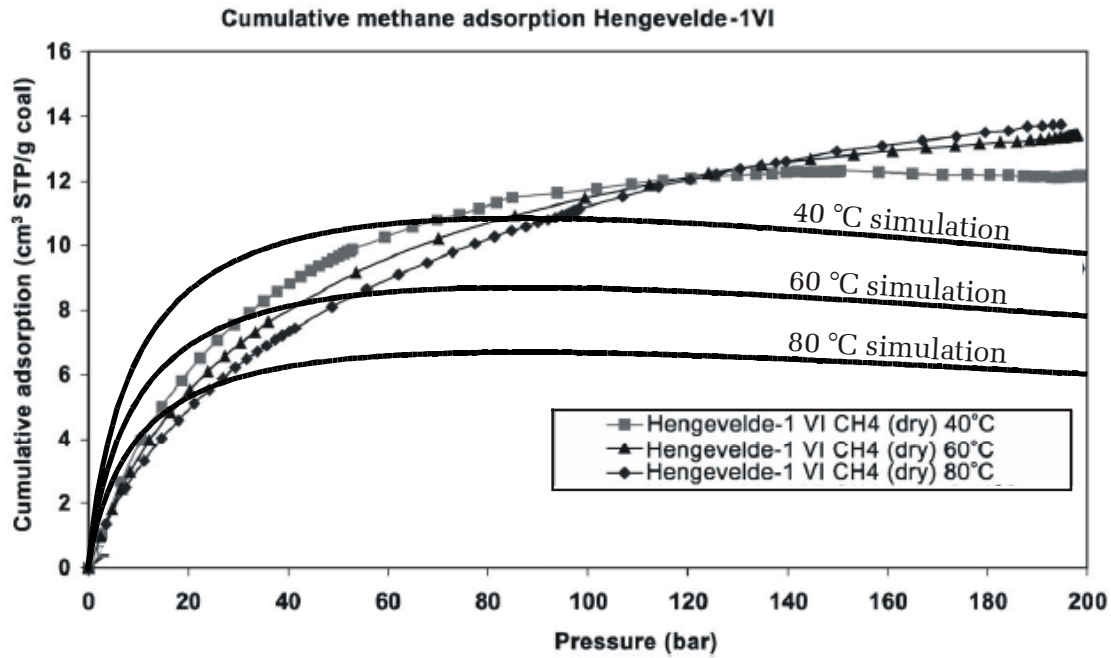


Figure 7:

Simulation of adsorption behaviour of CH<sub>4</sub> on coal for the Hengevelde-1VI coal sample, recalculated to excess sorption data. The experimental data obtained by [15] for this sample shown as background. The simulated 40 °C-data deviate significantly from the measurements, but yield realistic values. Those for higher temperatures are inaccurate at higher pressures, probably due to the lack of data available for calibration (see fig. 5).

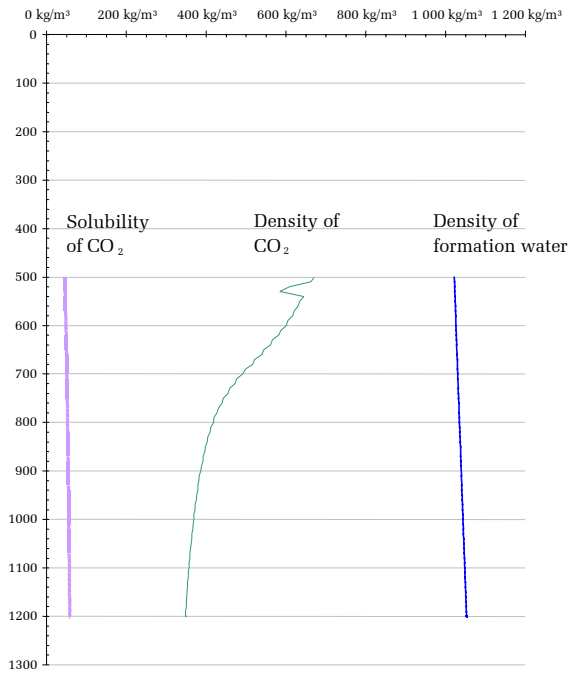


Figure 8:

The density of CO<sub>2</sub> in a dry reservoir, compared to the solubility of CO<sub>2</sub> in a flooded reservoir. Both values are given in kg/m<sup>3</sup>, and the density of formation water is given for reference. Depth in metres.